Numerical simulation of diffusion in porous media using the Lattice Boltzmann Method

Mehdi Ayouz, Patrick Perre

Numerical simulation of diffusion in porous media using the Lattice Boltzmann Method

Mehdi Ayouz and Patrick Perré

Ecole Centrale Paris
Laboratoire de Génie des Procédés et Matériaux (LGPM)
Grande Voie des Vignes
Châtenay-Malabry, France
mehdi.ayouz@ecp.fr;patrick.perre@ecp.fr

ABSTRACT. *A numerical simulation of the diffusion phenomenon was carried out in heterogeneous porous mediausing the Lattice Boltzmann method. The developed code was tested on a rectangular lattice divided in two subdomains, each of them associated to a thermal conductivity. Once validated, the code was used to compute the equivalent thermal conductivity of the cellular structure of spruce. The simulation was done in the two transverse direction of wood (radial and tangential). The computed equivalent thermal conductivities in tangential and radial direction are quite close to the theoretical values obtained for the same phases placed in parallel. These results are in good agreement with pervious works and then represent the first step for modeling the mass and thermal diffusion coupling through a three-dimensional heterogeneous porous media.*

KEYWORDS: Lattice Boltzmann, Porous media, Conductivity, Diffusion, Simulation, Heterogeneous.

1. Introduction

The Lattice Boltzmann Method (LBM) was first developed to solve the macroscopic momentum equation for viscous flows (Succi 2001). Based on velocities distributions on a regular lattice, this method simulates the macroscopic behavior as an emerging property of the discrete movement of particles (propagation and collision). Indeed, an asymptotic development of the lattice rules allows the macroscopic set of equations to be theoretically derived from the discrete rules. Following this strategy, LBM progressively became a general numerical method able to solve any kind of partial differential equations. It belongs to the family of so-called meshless methods (Belytschko et al. 1996, Frank and Perré 2010) and therefore has interesting properties such as simplicity of development, suitable to parallel computing, flexibility in geometrical shape.

In this work, we used this method to solve diffusion in heterogeneous media. The adaptation of LBM to diffusion in heterogeneous media is first briefly described. A

validation of this principle is then proposed for the simple case of two contrasted phases placed in parallel. Finally, we applied the code to compute the equivalent properties of a typical cellular arrangement found in softwood. In this case, an image-based lattice generation is used to define the phase morphology.

2. Materials and Methods

2.1. The Lattice Boltzmann Model

In the standard Lattice Boltzmann (LB) model, the single-particle distribution function obeys to the following equation

$$f_i(\vec{x} + \vec{c}_i\delta t, t + \delta t) - f_i(\vec{x}, t) = \Omega_i(\vec{x}, t) \quad (1)$$

Where $\vec{c}_i$, is the discrete particle velocity vector and $\Omega_i(\vec{x}, t)$ is the collision term. The set of vectors $\vec{c}_i$ are the possible velocities a particle can move from a lattice site to a nearest-neighboring site at each time step $t + \delta t$. For simplicity, we used a "single relaxation time" form for the collision term

$$\Omega_i(\vec{x}, t) = -\frac{1}{\tau}\left[f_i(\vec{x}, t) - f_i^{eq}(\vec{x}, t)\right] \quad (2)$$

Where τ is the mean collision time and $f_i^{eq}(\vec{x}, t)$ are the equilibrium distribution functions at site $\vec{x}$ and time t. The above equation is well known as the BGK (Bhatnagar-Gross-Krook) approximation for the collision operator $\Omega_i(\vec{x}, t)$. This means that after collision the distribution function tends to an equilibrium Maxwell-Boltzmann distribution.

In the present work, a standard D2Q9 model was adopted, i.e. a two-dimensional computational domain (x, y) involving 9 discrete velocities; $c_i \ \forall\, i = \{0,1, \dots 8\}$. These velocities are defined (see Fig.1.a) as follows

$$\vec{c}_i \begin{cases} c_i(0,0) & i = 0 \\ c_i(\pm 1,0), c_i(0,\pm 1) & i = 1,2,3,4 \\ c_i(\pm 1,\pm 1) & i = 5,6,7,8 \end{cases} \quad (3)$$

Where $c = \frac{\delta x}{\delta t} = \frac{\delta y}{\delta t}$, δx and δy are the lattice spaces and δt the lattice time step size.

For a diffusion problem, it is appropriate to consider the equilibrium distribution function as constant, where no macroscopic velocity is involved. This can be formulated as follows

$$f_i^{eq}(x, y, t) = \omega_i \theta(x, y, t) \quad (4)$$

Where ω_i are the weighting factors and $\theta(x, y, t)$ is the normalized macroscopic temperature field such as: $\theta(x, y, t) \in [0,1]$. In the D2Q9 model, the weighting factors are given as

$$\omega_i \begin{cases} 4/9 & i = 0 \\ 1/9 & i = 1,2,3,4 \\ 1/36 & i = 5,6,7,8 \end{cases} \quad (5)$$

In Figure 1.b the discrete particle velocities are represented in a computational domain. For this example, the computational domain $[x_1, x_n] \times [y_1, y_n]$ was divided into two equal subdomains, $\Sigma_1 = \left(\frac{x_n}{2} \times y_n\right)$ and $\Sigma_2 = \left(\frac{x_n}{2} \times y_n\right)$. The LB equation (Eq.1), including the BGK approximation (Eq.2), can be reformulated as follows:

$$f_i(x+\delta x, y+\delta y, t+\delta t) - f_i(x,y,t) = \begin{cases} -\frac{1}{\tau_1}\left[f_i(x,y,t) - f_i^{eq}(x,y,t)\right] & \forall (x,y) \epsilon \Sigma_1 \\ -\frac{1}{\tau_2}\left[f_i(x,y,t) - f_i^{eq}(x,y,t)\right] & \forall (x,y) \epsilon \Sigma_2 \end{cases} \quad (6)$$

Where τ_1 and τ_2 are the mean collision times depending on the values of λ_1 and λ_2 for domain 1 and 2 respectively.

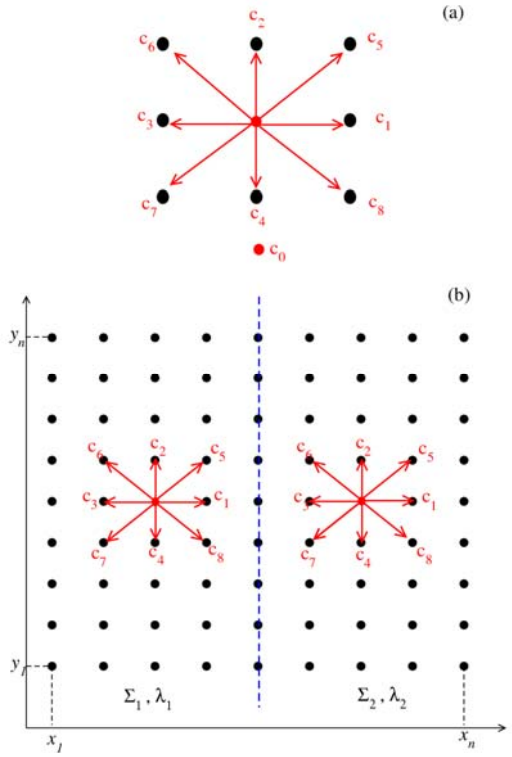

Fig. 1. (a) The discrete velocity vectors for D2Q9 model. (b) The computational domain used for validation, with subdomains Σ_1 and Σ_2*(separated by a dashed line) having thermal conductivity values,* λ_1*and*λ_2 *respectively. The lattice size is* $[x_1, x_n] \times [y_1, y_n]$.

2.2. The simulated configuration

The configuration computed in the present work consists of a diffusion problem inside a 2-D rectangular porous medium. Initially $(t = 0)$, a constant temperature, $\theta(x, y, t = 0) = 0$ is assumed. Along the x-direction, Dirichlet boundary conditions were applied: $\theta(x = x_1, y, t) = 1$ at x_1 and $\theta(x = x_n, y, t) = 0$ at x_n. To obtain a 1-D solution,

adiabatic conditions were set along the y-direction: $q(x, y = y_1, t) = 0$ and $q(x, y = y_n, t) = 0$.

The standard two–dimensional diffusion equation for the normalized temperature field

$$\frac{\partial \theta}{\partial t} = \frac{\rho c_p}{\lambda}\left[\frac{\partial^2 \theta}{\partial x^2} + \frac{\partial^2 \theta}{\partial y^2}\right], \tag{7}$$

was solved, using the LB model. In the above equation, ρ and c_p are the density and the heat specific capacity, respectively. The ratio $\rho c_p/\lambda$ representing the macroscopic diffusion coefficient is assumed to be constant.

In the literature (Higuera 1990), it has been demonstrated that using Chapman-Enskog expansion for the LB equation (Eq.1 including Eq.2), the diffusion equation can be derived. The relationship between macro and meso-scales gives:

$$\frac{\rho c_p}{\lambda} = \frac{1}{3}\left(\tau - \frac{\delta t}{2}\right) c^2 \quad \forall\, \Sigma_1, \Sigma_2 \tag{8}$$

Where τ has a dimension of time, i.e. is expressed in seconds. The macroscopic normalized quantities, such as temperature θ and flux φ, are obtained through moment summations in the velocity space:

$$\theta(x, y, t) = \sum_i f_i(x, y, t) \tag{9}$$

$$\vec{\varphi}(x, y, t) = \sum_i \vec{c}_i f_i(x, y, t) \tag{10}$$

Since a unit ratio of ρc_p between Σ_1 and Σ_2 is assumed, the normalized fluxes have the following forms

$$\vec{q}(x, y, t) = \begin{cases} \frac{\left(\tau_1 - \frac{1}{2}\right)}{\tau_1}\vec{\varphi}(x, y, t) \;\; \forall (x, y) \epsilon \Sigma_1 \\ \frac{\left(\tau_2 - \frac{1}{2}\right)}{\tau_2}\vec{\varphi}(x, y, t) \;\; \forall (x, y) \epsilon \Sigma_1 \end{cases}, \tag{11}$$

3. Computational implementation

In the LB formalism, equation (6) consists of two steps, collision and streaming. The distribution functions out of the domain at x_1, x_n, y_1 and y_n are known from the streaming process and the unknown distribution functions are towards the domain. For example the distribution functions (f_1, f_5, f_8) and (f_3, f_6, f_7) associated to velocities (c_1, c_5, c_8) and (c_3, c_6, c_7) in Fig.1.b are known at the lattice sites x_1 and x_n, respectively. In contrast, (f_3, f_6, f_7) at x_1 and (f_1, f_5, f_8) at x_n are unknown. For more details, see references (Bao *et.al*. 2008, Hao and Cheng 2009, Mohamad and Kurzmin 2010) and therein.

According to (Bao *et.al*. 2008) works, the implemented Dirichlet conditions can be expressed for the unknown distribution functions as follows

$$f_i(x_1, y, t) = \omega_i \theta_1 \quad \forall\, i = \{1,5,8\}$$

$$f_i(x_n, y, t) = \omega_i \theta_n \quad \forall\, i = \{3,6,7\}$$

Where θ_1 and θ_n are a fictive variables obtained from balance equations. In our case we used

$$\theta_1 = \frac{1}{\sum_i \omega_i}\left[\theta(x_1, y, t) - \left(\sum_{k=0}^{8} \tilde{f}_k(x_1, y, t) - \sum_i \tilde{f}_i(x_1, y, t)\right)\right] \quad \forall\, i = \{1,5,8\}$$

and

$$\theta_n = \frac{1}{\sum_i \omega_i}\left[\theta(x_n, y, t) - \left(\sum_{k=0}^{8} \tilde{f}_k(x_n, y, t) - \sum_i \tilde{f}_i(x_n, y, t)\right)\right] \quad \forall\, i = \{3,6,7\}.$$

Where $\tilde{f}_k$ and $\tilde{f}_i$ represent the distribution functions after collision and streaming, and k an index running over all velocities. Notice that i runs only over the unknown velocities indexes.

For the adiabatic boundaries, the unknown distribution functions can be obtained by a first order interpolation such as

$$f_i(x, y_1, t) = \tilde{f}_i(x, y_2, t) \quad \forall\, i$$
$$f_i(x, y_n, t) = \tilde{f}_i(x, y_{n-1}, t) \quad \forall\, i$$

Where n is the lattice at the boundary and $n-1$ is the lattice in the domain to the boundary lattice.

A FORTRAN custom code was developed using the following algorithm:

i. Calculate the equilibrium density function.
ii. Perform the collision procedure including lattice sites at the boundaries.
iii. Stream the density distribution populations.
iv. Apply boundary conditions for density distribution function.
v. Calculate macroscopic temperature and flux.

4. Results and discussion

First we used the code to simulate a diffusion phenomenon in a 100×100 lattice divided in two subdomains (Σ_1, Σ_2) as shown in Fig.1.b, composed of solid and gas, respectively. The solid fraction $\varepsilon_s$was equal to 0.5 and the thermal conductivity of solid and gas were set to $\lambda_1 = 1$ and $\lambda_2 = 0.0223$. This large contrast of thermal conductivities was used to test the consistency of the code. For convenience, the lattice lengths (x, y) were normalized to unity.

Figure 2 depicts the temperature profile along the x-direction at $y = y_n/2$. It represents the evolution of the 1-D temperature field from the unsteady state (dashed lines) to steady state regime (full line), for different calculation times. At short times, classical transient temperature profiles are obtained, those of a semi-infinite and uniform medium with uniform initial field and sudden change imposed on one face due to the Dirichlet condition. Once the thermal perturbation attains the mid-width of the medium (green line), the effect of conductivity contrast becomes obvious. The equilibrium temperature

profile is consistent with the simple analytical solution in a slab of finite thickness, with two phases placed in series and submitted to different Dirichlet conditions.

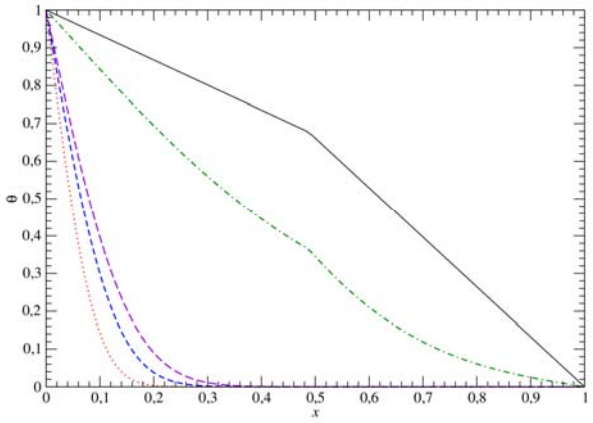

Fig. 2. (Color online) One-dimensional temperature profile along x-direction at $y = y_n/2$. *Different profiles are represented going from unsteady to steady-state regime. Notice that* $x = 0.5$ *is the separation between the both subdomains* Σ_1 *and* Σ_2

In addition to the temperature behavior, the one dimensional flux profile for the same time calculations is represented in Fig. 3. These curves confirm the progressive evolution of the system towards its equilibrium. Note that the contrast of conductivities is not directly visible on the flux, as the conservation law of energy imposes the flux continuity. This is particularly obvious at equilibrium, where the temperature profile allows the boundary between the two subdomains to be easily detected while the flux profile is perfectly flat (inset of Fig. 3).

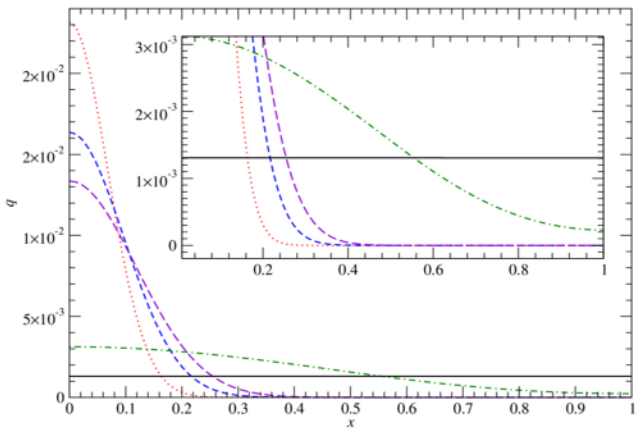

Fig. 3. (Color online) One-dimensional flux profile along x-direction at $y = y_n/2$. *Different profiles are represented going from unsteady to steady-state regime. The inset zooms the flux profile on the small magnitude region. (Elapsed times are the same as those displayed in Fig. 2).*

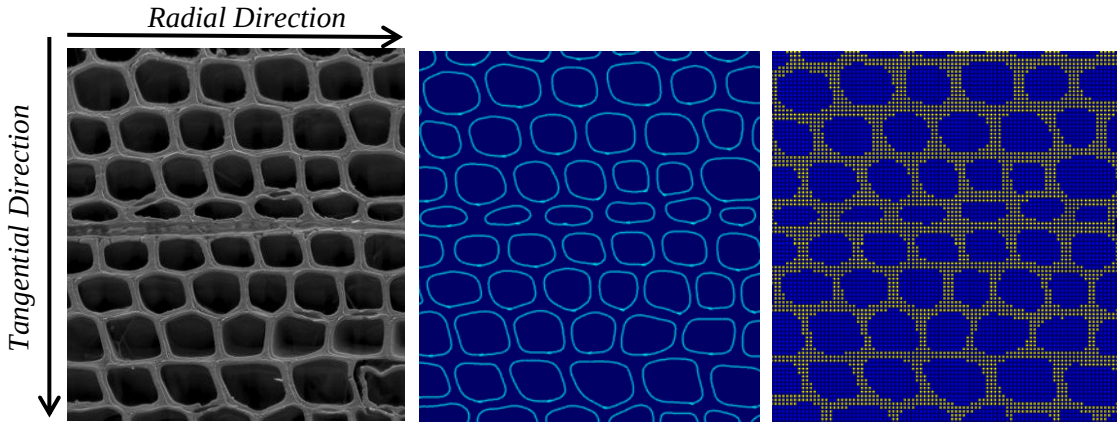

Fig. 4. (Color online) Image-based lattice generation: from an ESEM image of spruce, to lumen contours and computational lattice ($\varepsilon_s = 0.4$).

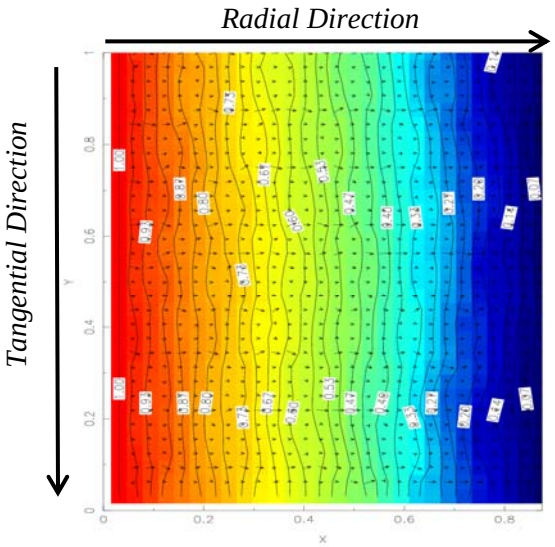

Fig.5. (Color online) The two-dimensional steady-state temperature profile and thermal flux (cellular structure, flux in the radial direction).The arrows represent tangential and radial directions.

Once validated, the model is used to compute the equivalent thermal conductivity of the cellular structure of spruce. For this purpose, an image-based lattice generation is used to define the phase morphology thanks to the custom software *MeshPore* (Perré, 2005). Figure 4 summarizes the main steps from image to the heterogeneous lattice and figure 5 depicts the field of temperature and thermal flux obtained in steady-state regime.

The simulation was done in the two transverse directions of wood (radial and tangential), which means,respectively,a flux along the horizontal and vertical directions of the image depicted in figure 4. We obtained an equivalent thermal conductivity of 0.234 and 0.281 $W.m^{-1}.K^{-1}$ in tangential and radial direction respectively. These values are quite close to the theoretical value obtained for the same phases placed in parallel (0.413), compared to the series model (0.036). Due to the way wood is formed in trees, the radial cell walls are rather placed in parallel along the radial direction, which explains the slightly higher

conductivity in that direction. All these values are in good agreement with previously published works (Perré and Turner, 2001).

5. Conclusion

In this work, a Lattice Boltzmann code was developed to simulate the diffusion phenomenon in heterogeneous porous media. The code was firstly tested on a rectangular lattice divided in two subdomains, each of them associated to a thermal conductivity. Once validated, the developed code was used to compute the equivalent thermal conductivity of the cellular structure of spruce, in the two transverse direction of wood (radial and tangential). The obtained conductivities are quite close to the theoretical ones and in good agreement with pervious works. These results represent the first step for modeling the mass and thermal diffusion coupling through 3-D heterogeneous porous media.

6. References

Bao J. , Yuan P., Schaefer L., A mass conserving boundary condition for the lattice Boltzmann equation method, Journal of Computational Physics 227,2008, 8472 8487.

Belytschko,T., Krongauz Y., Organ D., Fleming M., Krysl P., Meshless Methods: An Overview and Recent Developments. Computer Methods in Applied Mechanics and Engineering 1996, 139: 3-48.

Frank X., Perré P., The potential of meshless methods to address physical and mechanical phenomena involved during drying at the pore level, Drying Technology, 2010, 28: 932-943.

Hao L., Cheng P., Lattice Boltzmann simulations of anisotropic permeabilities in carbon paper gas diffusion layers, Journal of Power Sources 186, 2009, 104-114.

Higuera F. J., Lattice gas method based on the Chapman-Enskog expansion, Physics of fluids A, June 1990.

Mohamad A.A., Applied Lattice Boltzmann Method for Transport Phenomena, Momentum, Heat and Mass Transfer, Sure Print, Calgary, 2007.

Mohamad A.A., Kuzmin A., Acritical evaluation of force term in lattice Boltzmann method, natural convection problem, International Journal of Heat and Mass Transfer 53, 2010, 900-996.

Perré P., *MeshPore* : a software able to apply image-based meshing techniques to anisotropic and heterogeneous porous media, Drying technology Journal, 2005, 23: 1993-2006.

Perré P., Turner I., Determination of the material property variations across the growth ring of softwood for use in a heterogeneous drying model. Part II : use of homogenisation to predict bound water diffusivity and thermal conductivity, Holzforschung, 2001, 55: 417–425.

Succi S., The Lattice Boltzmann Equation for Fluid Dynamics and Beyond. Clarendon Press, Oxford, 2001.